Beach tar accumulation, transport mechanisms, and sources of variability at Coal Oil Point, California

Tonya S. Del Sontro [a,*], Ira Leifer [a], Bruce P. Luyendyk [b], Bernardo R. Broitman [c]

[a] *Marine Science Institute, University of California, Santa Barbara, CA 93106, USA*
[b] *Department of Earth Sciences, University of California, Santa Barbara, CA 93106, USA*
[c] *National Center for Ecological Analysis and Synthesis, University of California, Santa Barbara, CA 93101, USA*

Abstract

A new field method for tar quantification was used at Coal Oil Point (COP), California to study the mechanisms transporting oil/tar from the nearby COP natural marine hydrocarbon seep field. This method segregates tar pieces into six size classes and assigns them an average mass based on laboratory or direct field measurements. Tar accumulation on the 19,927 m^2 survey area was well resolved spatially by recording tar mass along twelve transects segmented into 4-m^2 blocks and then integrating over the survey area. A seasonal trend was apparent in total tar in which summer accumulations were an order of magnitude higher than winter accumulations. Based on multiple regression analyses between environmental data and tar accumulation, 34% of tar variability is explained by a combination of onshore advection via wind and low swell height inhibiting slick dispersion.
© 2007 Elsevier Ltd. All rights reserved.

Keywords: Santa Barbara Channel; Tar; Seeps; Oil slick; Oil advection

1. Introduction

Most concern regarding oil pollution is focused on anthropogenic sources – i.e., oil extraction, transportation, and consumption. However, more than 60% of oil in North American waters and 45% globally come from natural marine hydrocarbon seeps (NRC, 2003). Marine seepage is hydrocarbon (gaseous and/or liquid phase) leakage from subsurface strata into the water column (Hunt, 1996). Among the most visible manifestations of marine oil in the environment is the formation and beach stranding of tar, which is the physically and chemically weathered remnant of an oil slick. Coastal tar accumulation is common on many California beaches due to chronic oil emissions from natural oil seeps in the petroliferous region (Mertz, 1959; Hartman and Hammond, 1981; Leifer et al.,

2006a). Hydrocarbon seeps exist off the coast of California from Santa Monica Bay through the Santa Barbara Channel to Point Conception and in Monterey Bay (Fischer, 1977; Henyey et al., 1977; Lorenson et al., 2002). Despite relevance to the quality of coastal life and its environmental impact, few beach studies regarding tar accumulation from natural seeps have been published.

Previous research has quantified beach tar accumulation as a result of an oil spill or beach stranding of pelagic tar (Iliffe and Knap, 1979; Romero et al., 1981; Golik, 1982; Richardson et al., 1987; Asuquo, 1991; Corbin et al., 1993; Sen Gupta et al., 1993; Gabche et al., 1998; Owens et al., 2002). Although some of these studies had high temporal resolution, spatial resolutions generally were very low and inconsistent. Most studies surveyed a few narrow transects at various beaches over a large stretch of coast or a single line parallel to shore, while others surveyed random transects, potentially introducing bias. Some beach tar studies were conducted following an oil spill and thus, only lasted the duration of high tar/oil stranding. Other studies were conducted in coastal areas or on islands in proximity

to shipping lanes or ports and recorded relatively low pelagic tar accumulations.

The majority of these studies used similar observational methods, such as recording random tar piece diameters and weight or estimating percent oil/tar cover in an area (Owens et al., 2002). The shoreline cleanup assessment team (SCAT) procedure was developed in order to standardize tar surveys for cleanup agencies (Owens, 1999). This method involves surveying along random transects parallel to shore and averaging the number and size of tar pieces on transects. SCAT procedures provide useful information regarding coastal tar accumulation for the purposes of cleanup, but they do not systematically quantify beach tar with high spatial resolution for the purposes of understanding processes leading to tar accumulation.

Few field studies have addressed the processes by which marine oil reaches the coast. Iliffe and Knap (1979), Shannon et al. (1983), Otero et al. (1987), and Corbin et al. (1993) suggested that much of the variability in the spatial tar distribution was due to the beach location and orientation relative to dominant current and wind patterns. Another potentially important source of variability was the presence and location of shipping lanes. Oil slick models, which largely are based on laboratory results, incorporate many of the physical, chemical, and biological transport and weathering processes that act upon oil at sea (Reed et al., 1999). In general, currents, wind, and waves or swell are the dominant processes in long distance oil slick advection or transport, particularly offshore. Other processes are important in coastal zones, but generally are not incorporated in oil slick models. For example, wave breaking in the surf zone and wave-induced alongshore currents affect shoreline stranding (Reed et al., 1999). Also, tides may be important – Hartman and Hammond (1981) observed that beach tar had a residence time of 1–2 tidal cycles; thus, tides can directly affect measurements of tar mass and estimates of beach tar flux.

This paper describes a new and robust sampling protocol for quantifying beach tar accumulation. We used this method to systematically measure tar accumulation throughout 2005 at Coal Oil Point (COP), California, which is adjacent to one of the largest natural marine hydrocarbon seep fields in the world (Hornafius et al., 1999). The resulting tar accumulation time series was analyzed with respect to environmental parameters that could potentially influence beach tar accumulation. Analysis allowed better understanding of the causes of variability in tar accumulation and identified some of the important processes controlling oil transport in nearby coastal waters to the study site.

1.1. Study area

The study area, COP beach, has the most heavily concentrated tar accumulation along the United States west coast (Mertz, 1959). COP is a south-facing point in the Santa Barbara Channel (SBC) adjacent to the COP seep field (Fig. 1). Oil and gas escape to the ocean from the Miocene Monterey Formation reservoir underlying the SBC. The COP seep field is one of the most prolific (Landes, 1973) and extensively studied marine seepage areas in the world. Studies over the past few decades provide much insight into the temporal and spatial variations in seepage distribution and flux (Allen et al., 1970; Fischer and Stevenson, 1973; Hornafius et al., 1999; Quigley et al., 1999; Leifer and Boles, 2005, 2004; Washburn et al., 2005; Leifer et al., 2006b). The current consensus is a range of $1–2 \times 10^5$ m^3 CH$_4$ dy^{-1} from the COP seep field (Hornafius et al., 1999). Oil emissions were estimated at a minimum of 100 barrels day^{-1}, (Clester et al., 1996; Hornafius et al., 1999), although significant variability exists on a range of time scales.

A few studies have geochemically characterized California beach tar in an effort to identify sources (Hartman and Hammond, 1981; Kvenvolden et al., 2000; Hostettler et al., 2004). Hartman and Hammond (1981) distinguished between various natural seep oil sources of beach tar using carbon and sulfur isotopes and estimated that 55% of Santa Monica beach tar was from the COP seep field, over 250 km to the west. Tar primarily accumulated during the spring, summer, and autumn months. They proposed that during spring and summer COP seep oil exits the SBC to the west and is transported south and east towards Santa Monica Bay by the southerly California Current. They proposed that during winter months the northerly Davidson Current surfaces at the western boundary of the SBC and transports COP seep oil north. Leifer et al. (2006a) looked at physical advection and chemical evolution of oil slicks within the seep field, but did not investigate transport to beaches. In fact, no published studies have identified the transport mechanisms by which COP seep oil/tar reaches
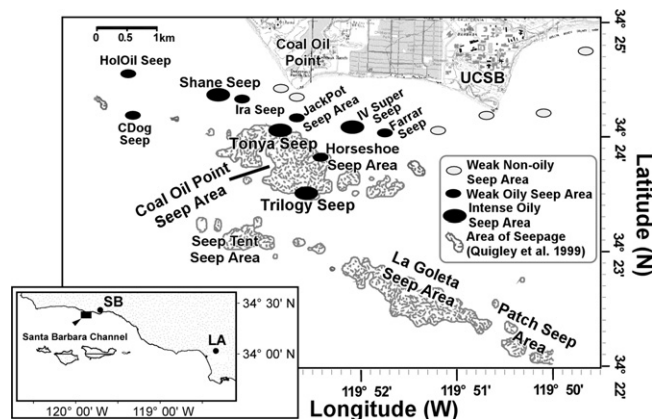

Fig. 1. Overview of the Coal Oil Point seep field, near University of California, Santa Barbara (USCB). Gray regions are areas of high bubble density as detected by sonar returns (Quigley et al., 1999). Informally named oily seeps are noted. Length scales and key on figure. "Weak" and "Intense" are qualitative descriptors for flux. Markers represent seepage areas containing multiple vents, not single vents. Inset shows southern California with study area indicated by small box in the Santa Barbara Channel. SB is Santa Barbara and LA is Los Angeles.

the shore and that influence its spatial or temporal distribution.

Unlike beach tar accumulation studies associated with oil spills or on beaches near heavy ship traffic, which generally have a transient source, natural seepage is a long-term chronic oil spill, albeit with variability in emissions on time scales from tidal (Leifer and Wilson, 2007) to decadal (Boles et al., 2001). Very few studies have investigated seep-related beach tar accumulation, although NOAA – the National Oceanic and Atmospheric Administration – listed this type of research as number one priority in regards to long-term oil weathering research (Mearns and Simecek-Beatty, 2003). A 2-year long tar survey of Santa Barbara County beaches (including COP) found that COP regularly accumulated more tar than any other studied beach by several orders of magnitude. They determined that all tar pieces collected were from the Monterey Formation oil and that concentrations were highest during summer and autumn months (Lorenson et al., 2004).

2. Methods

The experimental approach involved counting tar pieces in six size classes, $S(1-6)$, along a series of north-south transect lines, X_1-X_{12}, perpendicular to the bluffs (Fig. 2). Transect lines were evenly spaced 20-m apart at the bluff with X_6 centered on the point and covered a total area of 19,927 m^2. Tar pieces were counted in 2-m square quadrats (4-m^2 area blocks) along each transect line, extending from the bluff, Y_0, to the water line Y_n. To ensure repeatability of the location of transect lines, rebar was hammered into the sand at the base of the bluffs. The rebar defined Y_0, the top of each transect.

Tar mass was calculated from the tar counts using a functional relationship between tar size and mass. Counted tar mass was integrated over the survey area to yield total accumulated tar mass, M, which accounted for the irregular grid shape. In order to understand how environmental factors modify beach tar accumulation, the time series of total tar mass throughout the study, $M(t)$ where t is time, was related to oceanographic and meteorological parameters, including swell, currents, wind, and sea temperatures.

2.1. Tar quantification

Beach tar size classes were based on their surface area, specifically the approximate diameter of the longest surface dimension (Table 1; Fig. 2a). Typically, the surface cross-sections of tar pieces were circular to elliptical, allowing size classification within a set range of diameters. $S(1-5)$ had defined surface areas, while $S(6)$ was a catch-all class for tar pieces larger than $S(5)$.

To convert tar size counts into tar size mass, m_s, 100 representative tar pieces for $S(1-4)$ were collected and the mass of each was measured. Each tar piece was collected on aluminum foil and weighed on a digital scale. Then, each tar piece was dissolved through filter paper with dichloromethane leaving sand grains and other debris, which had been aggregated into the tar, stranded on the filter paper. The sand and debris were placed back on the original aluminum foil, weighed, and subtracted from the initial mass measurement. The average tar mass for $S(1-4)$, $\langle m_{1-4} \rangle$, allowed calculation of total tar mass observed for those size classes (Table 1).

$S(5)$ and $S(6)$ were treated differently. In the field, the three dimensions of each tar piece were recorded (length, width, and thickness) and the tar mass calculated based on a box volume model of tar shape and an assumed tar density, ρ_t, of 1.00 g cm^{-3}. Beach tar densities must be within a narrow range, between that of COP seep oil (0.9861–0.9953 g cm^{-3}; Jokuty et al., 1999) and seawater (1.025 g cm^{-3}), else the asphalt would sink and thus not float to the beach. As a result, actual tar densities should be within 1–2% of 1.00 g cm^{-3}, which was far less than the typical observed variability in $M(t)$. The average mass for $S(5)$ was calculated from the mass of all $S(5)$ tar pieces observed in the field (Table 1). The average mass of $S(6)$
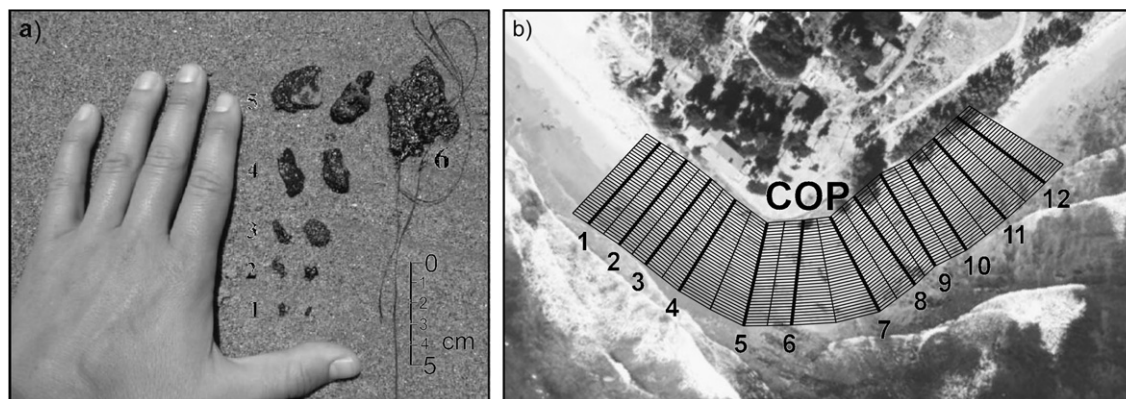

Fig. 2. (a) Tar balls were segregated into six size classes and counted along (b) twelve transects around Coal Oil Point (COP). Thick lines perpendicular to shore are transect centers (X_{1-12}). These lines parallel to those are transecting boundaries. Thin lines parallel to shore are the boundaries of transect segments (34 segments for each transect. Y_{1-34}).

Table 1
Properties of tar ball size classes

Size class	D (cm)	$\langle m_s \rangle$ (g)	$\langle h \rangle$ (cm)	$\langle r \rangle$ (cm)	$\langle k \rangle$ (cm)	Count (%)	Mass (%)
$S(1)$	0.25	0.006 ± 0.004	0.122	0.125	0.182	53.38	4.27
$S(2)$	0.50	0.022 ± 0.011	0.112	0.250	0.280	33.23	9.75
$S(3)$	1.00	0.073 ± 0.037	0.093	0.500	0.418	9.60	9.35
$S(4)$	2.00	0.169 ± 0.096	0.054	1.000	0.553	3.05	6.87
$S(5)$	3.00	5.960 ± 7.444	0.405	1.500	1.327	0.54	21.31
$S(6)$	>4.00	25.82 ± 50.96	0.533	>2.00	2.220	0.21	48.45

S: size class; D: the approximate diameter; m_s: tar ball mass per size class; h: thickness; r: radius; k: characteristic length; $\langle \rangle$ denotes average.

was calculated in the same manner as $S(5)$, but is not a meaningful value because $S(6)$ does not have a defined size range.

Prior to 11 April 2005, data were collected only for transects X_{1-10}. A consistent peak in mass was noted at the eastern edge of the study area, X_{10}. Consequently, two eastern transects, $X_{11,12}$, were added to the study area to resolve the observed peak. The study area size was chosen to allow survey completion in less than half a tidal cycle (~3 h). For surveys prior to 11 April 2005, tar counts for transects $X_{11,12}$ were extrapolated based on the ratio of tar counts for those transects to the other 10 transects on surveys subsequent to 11 April 2005. Extrapolation allowed comparison of data before and after addition of the two transects.

2.2. Survey area integration

In order to calculate M, total tar mass throughout the study area, we integrated tar mass in each quadrat over the full survey area, accounting for the irregular geometry around Coal Oil Point. The conversion from a Cartesian coordinate system (X is transect, Y is quadrat) to a geographical map was based on the Global Positioning System (GPS) locations of the bluff and waterline ends of each transect line (Fig. 2b). Each transect extended 68 m from the bluff to the defined waterline. Data for each transect was considered representative of the beach spanning halfway between the two adjacent transects. Each transect was subdivided into 2-m segments along the Y-axis forming

34 segments, Y_1-Y_{34}. The width of each segment was the average of the distance to each adjacent transect. The area of each segment was calculated in square decimal-minute from half the determinant of the two triangles that form the rectangular segments and then converted into meter-squared using the meter distance between a minute latitude and minute longitude at 34°N, 119°W.

2.3. Environmental forcing analysis

To identify transport processes related to variations in tar accumulation, several environmental data were acquired for the study period (see Table 2). Parameters hypothesized as potential environmental forcing factors were analyzed individually by comparing their temporal trends with that of $M(t)$ and calculating Pearson correlation coefficients (Sokal and Rohlf, 1995). These factors included the east-west component and north-south component of surface currents (as measured by CODAR – Coastal Ocean Dynamics Application Radar) and winds, significant swell height and direction, sea bottom (SBT) and sea surface temperatures (SST).

To examine patterns of association over a range of temporal scales, we also conducted cross-correlations by lagging the environmental records every 2 h and up to 24 h prior to the survey time. Lagged correlations were performed on raw environmental data as preliminary analyses showed a lack of correlation between tar accumulation and data filtered over 12, 18, and 24 h with inconclusive results for 6-hour filtered data. A Bonferroni correction (Sokal

Table 2
Environmental data sources

Factor	Source	Location (34°, 119°)	Dist. (km)	Direction	Sampling time (min)
Wind (http://www.sbcapcd.org/Default.htm)	SBCAPCD	24′55″N, 52′43″W	0.9	NW	5
Swell/SST (http://cdip.ucsd.edu/)	CDIP (Buoy #107)	20′6″N, 8′12″W	10	SE	30
SBT (http://sbc.lternet.edu/)	SB LTER Naples ADCP (16 m)	25′25″N, 57′1″W	7	W	20
Currents (http://www.oceancurrentmaps.net/)	UCSB IOG (CODAR)	23′45″N, 53′14″W	1.5	SSW	60

SBCAPCD: Santa Barbara county air pollution control district; SST: sea surface temperature; CDIP: coastal data information program; SBT: sea bottom temperature; SB LTER: Santa Barbara long term ecological research; UCSB: University California, Santa Barbara; IOG: interdisciplinary oceanography group; CODAR: coastal ocean dynamic application radar; Dist: distance from Coal Oil Point; Direction: from Coal Oil Point.

and Rohlf, 1995) was used to adjust the significance level ($\alpha = 0.05$) in multiple comparisons. Finally, we combined the observed maximal lagged correlations between individual environmental variables and tar mass in a multiple linear regression model in order to propose a mechanistic model of environmental forcing of tar to COP. Correlation and regression analyses were performed on $\log(M(t))$.

3. Results

3.1. Tar size characteristics and distribution

The average mass, $\langle m_s \rangle$, and variability in $\langle m_s \rangle$ increased with tar size (Table 1). Because tar size segregation used only surface area, tar thickness, h, was a derived parameter. For $S(1–4)$, h was estimated using the volume, V, equation of an ideal cylinder ($V = f\pi r^2 h$), where f is the fraction to which the surface area is equivalent and r is radius. In this case,

$$h = V/f\pi r^2 = m/\rho_t f\pi r^2, \qquad (1)$$

where $m = \langle m_s \rangle$ when $\rho_t = 1.00 \text{ g cm}^{-3}$. A comparison of h to r shows that as tar pieces increase in surface area, they become thinner (Table 1). This method of determining h was unnecessary for $S(5)$ and $S(6)$ where h was directly measured. An average h was computed from the individual $S(5)$ and $S(6)$ thickness measurements and are significantly higher than h for $S(1–4)$ (Table 1).

A characteristic length, k, also was calculated for the size classes, where k is defined as $V^{(1/3)}$ and $V = \langle m_s \rangle/\rho_t$. k is the dimension for an idealized cubic tar piece and provides a single dimension for each size class. Mean k for $S(5)$ and $S(6)$ was calculated from individual values of k based on the measured tar piece dimensions. A linear fit of k to r showed that tar thickness did not increase in proportion with surface area ($k = 1.0221r - 0.0856$, $r^2 = 0.9169$) – i.e., tar piece surface area increased with size class at a faster rate than tar thickness. Our defined tar size classes, $S(1–5)$, included over 99% of the tar pieces observed and over 51% of tar mass observed (Table 1). $S(6)$ tar provided the remainder of mass observed but were much more rare (0.21% of observed tar).

3.2. Observed tar accumulation

COP tar accumulation was surveyed on 57 days from February through December 2005 (Fig. 3a) with 17, 14, 9, and 17 days during winter, spring, summer, and autumn, respectively. Zero tar was observed on only two winter days (24 February and 8 March). Non-zero values of M ranged from 0.10 kg (4 November) to 39.11 kg (27 February). For the entire study, mean M (steady state tar accumulation) was 4.40 kg.

Except for 27 February 2005, which for several reasons was unique (discussed in Section 4.2), tar accumulation data showed an overall seasonal cycle with M doubling from winter to spring and then roughly doubling again into
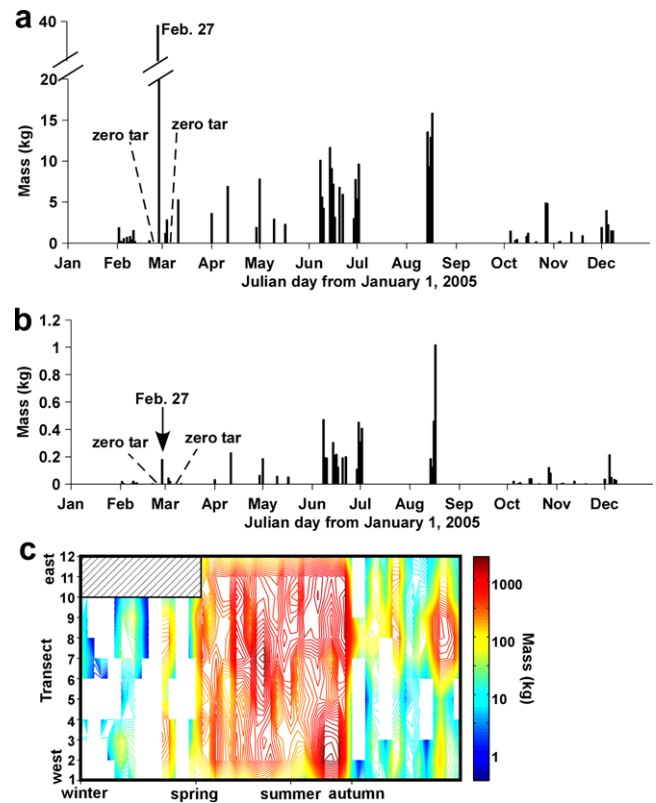

Fig. 3. (a) Total tar mass on 57 days during 2005. (b) Tar mass observed in four smallest size classes. (c) Total tar mass with respect to transect and survey (season transition noted below figure). Contour mass values indicated by color bar at right. Shaded region had no data; white areas represent zero tar accumulation.

summer, followed by a sharp decrease in autumn to M values comparable to winter (Fig. 3a). Further, the variation between seasons was much larger than the intra-season variability. Mean summer M was about an order of magnitude larger than mean winter M (excluding 27 February 2005; Table 3). Mean tar coverage for the study area varied from 0.052 g m^{-2} in winter (excluding 27 February) to 0.465 g m^{-2} in summer (Table 3). With 27 February, winter tar coverage was greater than autumn, but still lower than spring and summer.

The inter-seasonal variability is readily apparent in the spatial tar accumulation distribution of $M(X,t)$ or mass per transect per day (Fig. 3c). Sharp transitions are clear across the entire survey area at the winter/spring and summer/autumn boundaries. Another notable difference is the many days during winter and autumn in which $M(X,t) = 0$ for some transects (white indicates zero tar in Fig. 3c). In contrast, $M(X,t)$ was always greater than zero during spring and summer surveys. Generally, transects during spring and summer had more than 500 g of tar, while winter transects typically had less than 50 g. Over half the autumn transects contained less than 50 g of tar, but a few transects had between 100 and 500 g and there were fewer tar-free transects during autumn compared to winter.

Table 3
Summary of seasonal tar accumulation

	Spring	Winter[a]	Winter[b]	Summer	Autumn
Days surveyed	14	17	16	9	17
$\langle M \rangle$ (kg)	5.97 ± 3.05	3.27 ± 9.33	1.03 ± 1.38	9.27 ± 4.22	1.66 ± 1.54
Mean coverage (g m^{-2})	0.300	0.164	0.052	0.465	0.083
$\langle M_{1-5} \rangle$ (kg)	3.20	0.521	0.346	6.20	1.04
$\langle M_{1-4} \rangle$ (kg)	2.02	0.209	0.102	4.00	0.467

$\langle M \rangle$: Mean tar accumulation (subscripts are tar size classes).
[a] With 27 February.
[b] Without 27 February.

3.3. Environmental forcing of tar accumulation

Oceanographic (surface currents, swell height and direction, sea surface and sea bottom temperatures) and meteorological (wind direction and speed) factors can affect M. These factors were compared to $M(t)$ with particular attention to seasonal variations.

Although u_w, the east-west component of the wind, was more or less constant throughout the year, v_w, the north-south component of the wind, showed a seasonal pattern (Fig. 4a). v_w was often positive (to the north) during spring and summer and negative (to the south) during autumn and winter.

Surface current speeds from the CODAR grid location closest to the COP seep field ranged widely, from less than
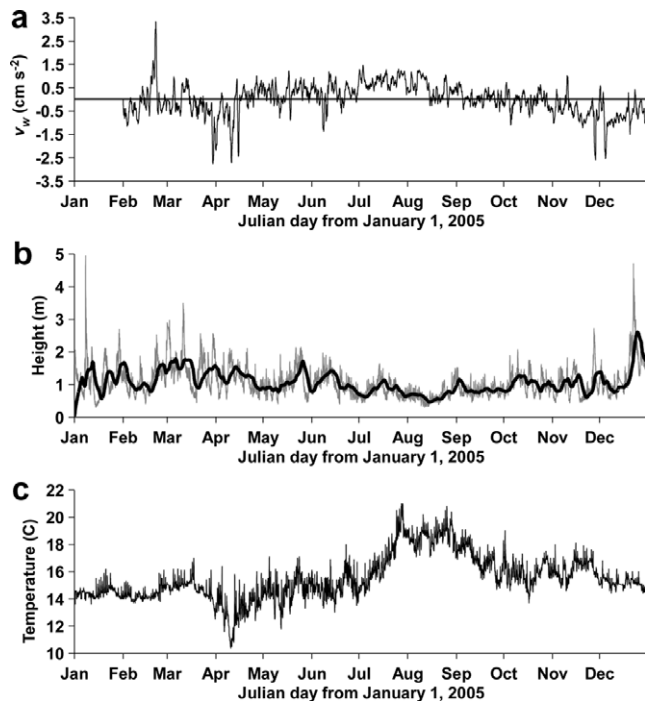

Fig. 4. (a) Daily mean of 10 m north-south wind component, v_w for 2005. Horizontal line at $v_w = 0$ marks boundary between winds to the north (positive) and winds to the south (negative). (b) Significant swell height in meters for 2005. Light gray and black lines are 30 min and 5-day resolutions, respectively. (c) Sea surface temperature (30 min resolution) during 2005.

1 to 60 cm s^{-1}, and the direction was to the WNW over 50% of the year. There was no apparent seasonal trend in u_c, the east-west current component, or v_c, the north-south current component.

Swell height typically was less than 1 m during late spring, summer and early fall and ranged from 1 to 2 m during late fall and winter (Fig. 4b). Thus, swell height trended inversely to $M(t)$. Swell direction was from the west more than 90% of the year.

The SST time series (Fig. 4c) appeared to follow $M(t)$, except for a sudden decrease and subsequent increase of temperature in April. SBT, recorded at 16 m of an 18-m deep water column, were similar to SST, including the mid-April decrease. SBT for the last 2 months of 2005 were missing from the dataset.

We found several environmental factors correlated with $M(t)$. Swell height was inversely related to $M(t)$ with no temporal lag ($r = -0.40$, $p = 0.002$). v_w showed a maximal positive correlation to $M(t)$ with a time lag of 14 h ($r = 0.35$, $p = 0.009$). The maximal lagged correlation between u_w and $M(t)$ was a positive one with a time lag of 18 h ($r = 0.35$, $p = 0.007$). A significant correlation was found between $M(t)$ and u_c at a time lag of 12 h ($r = 0.34$, $p = 0.009$). SBT was negatively and significantly correlated with $M(t)$ at all time lags ($r = 0.44$, $p = 0.001$). No significant correlation was found between $M(t)$ and v_c or SST for any time lag ($p > 0.05$).

We used swell height at zero lag, u_w with an 18-hour lag, and v_w with a 14 h lag in a multiple linear regression model. We selected these variables because they were orthogonal at those time lags – i.e., the variables were not correlated to each other. We found that u_c was significantly correlated with u_w and swell height. As CODAR measurements in the area have limited onshore resolution, we excluded them from the multiple regression model. In the case of SBT, it was significantly correlated with v_w and the record lacked two months of data, thus we also excluded SBT from the regression model. The multiple regression model with the three lagged, orthogonal and unfiltered environmental variables was highly significant ($R^2 = 0.34$, $p < 0.0001$, $F = 8.94$, d.f.e. = 53) and all regression coefficients were significant (for swell height, u-wind, and v-wind, $p = 0.006$, 0.0005, and 0.004, respectively).

4. Discussion

4.1. Tar size characterization

Estimating thickness, h, by the cylinder volume equation for $S(1–4)$ predicted a decreasing h with increasing surface area, which clearly disagreed with visual observations. The discrepancy probably lay in the assumption that tar piece cross-sections were circular ($f = 1$), which clearly was seldom true. Elliptical cross-sections were very common, especially among $S(3)$ and $S(4)$ tar pieces. h for $S(5)$ and $S(6)$ were measured directly and therefore fairly accurate.

The mass of $S(5)$ and $S(6)$, however, likely was overestimated by assuming tar pieces were best described by a box instead of a cylinder. For a circular cross-section tar piece, the box volume equation overestimates the cylinder volume value by 27%. Based on the contributions of $S(5)$ and $S(6)$ to the total mass (Table 1), this could have resulted in an upper limit overestimate of M by 6% and 13.5%, respectively. For most surveys, the overestimation likely was less because the true shape of $S(5)$ and $S(6)$ tar was in between these shapes. For the typical unequal length and width, the box volume model generally was more accurate than the cylindrical volume model.

Analysis of k showed that h increased with size class, but not in proportion to surface area. Visual tar observations during surveys confirmed this conclusion; h varied little between $S(1–6)$. This suggests that some physical process(es) inhibited thickening of tar pieces relative to surface area growth. Sun exposure is one possible process causing this. As the sun warms tar, whether on the sea surface or the beach, it becomes less viscous and tends to spread.

Overall, our tar size characterization method provided highly accurate mass estimates and covered the size range of tar pieces present on COP, such that each class contained a statistically significant number of tar pieces and the presence or absence of a $S(6)$ tar piece did not measurably affect total tar mass. Thus, this approach addressed a significant problem with lower spatial resolution surveys wherein random variability in the largest tar pieces affects the estimate of total beach tar. Moreover, a comparison of tar accumulation with respect to transect showed similar trends with and without $S(6)$ tar pieces.

4.2. Temporal tar variation

The observed seasonal beach tar trend at COP (higher in spring and summer) is similar to variations found in other studies (Hartman and Hammond, 1981; Lorenson et al., 2004). Importantly, this temporal variation was not solely determined by the mass contributions from the largest size classes, $S(5–6)$, where the statistics can be poor. The same seasonal trend is apparent in M_{1-4}, tar accumulation for $S(1–4)$ pieces (Fig. 3b), as well as in $\langle M_{1-5} \rangle$ (Table 3). February 27th also was exceptional in terms of winter $\langle M_{1-4} \rangle$ (Fig. 3b).

During the study, we estimated the tar residence time at between one and two tidal cycles depending on the phase of the lunar tidal cycle. Thus "bluff tar" could be counted multiple times on consecutive day surveys. Bluff tar was tar stranded at the top of the beach near the bluff following the highest high tide of a diurnal cycle. However, removal of bluff tar from the upper 8 m of each transect within the dataset reduced $M(t)$ by <10%, and $M(t)$ absent bluff tar showed the same seasonal patterns. Therefore, we concluded that bluff tar did not significantly affect the conclusions of this study.

M for 27 February was unique for several reasons. Not only was it the day of highest M during 2005, it also occurred during the season with the lowest $\langle M \rangle$ (Table 3). In fact, 27 February significantly skewed the mean winter mass by a factor of three. Inspection of the raw data showed that the exceptionally high M observed that day was real. We interpret this as an indication that the processes responsible for tar mass accumulation on 27 February were unique compared to those responsible for typical accumulation throughout the rest of the winter and possibly the entire year.

4.3. Environmental forcing of tar accumulation

The correlation and multiple regression analyses do not necessarily explain the seasonal variation in $M(t)$, but rather point out a set of environmental conditions that promotes tar accumulation at COP any time of the year. The analysis indicated that winds to the east 18 h prior to sampling, followed by winds to the north 4 h later (14 h lag), were conducive to high beach tar accumulation if the swell height was small at the time of sampling. As lagged correlations were performed every two h, the intervals provide a conservative approximation of the temporal window when environmental conditions may have promoted tar accumulation.

In addition, u_w was significantly correlated to $M(t)$ at other time lags, and thus winds to the east were important from 9 to 19 h prior to sampling. This time range is expected because environmental forcing is modulated by the parameter integrated over the requisite oil/tar transport time from the seep source to COP. Further, many environmental variables show strong diurnal and/or tidal cycles, such as winds and currents, respectively. Therefore, diurnal factors likely played a role in COP oil/tar transport.

Based on the multiple regression model, the set of conditions found that explains 34% of tar accumulation variability at COP during our study are consistent with the oceanographic setting of the northern SBC and orientation of COP relative to the oily seeps of the COP field. The majority of oily seeps lie between 0.5 and 3 km to the south of COP (Fig. 1). Other oily seeps are located further offshore to the southeast.

Surface currents act as a dominant oil advection mechanism, but tend to be more important in open water than in coastal environments (Reed et al., 1999). Generally,

currents off COP flow to the west completing the cyclonic gyre common to the SBC (Harms and Winant, 1998). Surface water trajectories from CODAR showed that during much of 2005 currents were to the WNW. Thus, when winds are light or out of the east, oil slicks originating from the seep field tend to travel west of COP (Fig. 5a).

The literature suggests that oil is advected at 3.5% of the 10-m wind speed plus the surface current velocity. Higher wind speeds cause wave breaking, which disperses oil slicks (Reed et al., 1999). In the coastal zone near COP, where winds and currents often are not aligned, the role of wind may be more significant than suggested. The multiple regression model suggests the following processes (as illustrated in Fig. 5 by a simplified schematic) are favorable for tar accumulation and occur more commonly in summer. First, currents advect oil westward and then a wind to the east directs the slick back towards COP (Fig. 5b) with subsequent winds to the north helping advect the slick onshore (Fig. 5c). Winds at COP generally were onshore (to the north) during spring and summer, which would increase beach tar accumulation, while the frequent offshore winds during winter and autumn would decrease tar accumulation (Fig. 4a).

Finally, intense surf zone activity affects beach tar in two manners. First, it disperses oil slicks into the water column, thus less oil/tar reaches the beach. Second, alongshore current induced by large swell would reduce the residence time of tar on the beach. Thus, when swell height is small, energy in the surf zone will be minimal and slicks will disperse less, while also increasing beach residence time. Swell height generally was smaller during spring and summer implying a weaker alongshore current and less surf zone activity.

These three conditions helped explain in part why tar accumulates so heavily during one season and not much during another. However, there was significant accumulation variation within a season. This variability is in part due to changes in the magnitude and direction of winds and currents. As illustrated in Fig. 5, even small changes

in u or v will change the angle that an oil slick travels, and thus the slick's impact upon the beach when it makes landfall. Further, certain acute angles would deposit more tar on one side of the point than the other, a close to perpendicular angle would deposit tar evenly along a wider swath of beach, and still at other angles, most of the tar would miss the survey area.

Another factor that is likely responsible for some of the accumulation is the tidal cycle. The three conditions and lag times selected for the multiple regression model leave $M(t)$ unexplained in terms of environmental conditions for ~12 h prior to sampling. During the 12 h prior to sampling, the beach experiences a complete cycle of one high and low tide. Observations showed that a flooding tide pushes tar further up the beach and depending on how much tar was left from the ebbing tide prior, tar will be present in the swash zone and perhaps at the top of the beach. An ebbing tide tends to remove some tar from the beach, but an onshore wind and/or a weak alongshore current will help strand tar on the beach as the tide is falling. During both tidal phases, some tar is most likely removed from the beach to open water. Although it seems intuitive that flooding tides bring in tar and ebbing tides remove it, the exact mechanism behind tar deposition and removal with respect to tides remains unclear.

Finally, the variability not explained by the multiple regression model and the observed intra-seasonal variability likely are due to source variability (discussed below), physical and chemical weathering processes, and additional oil transport processes (such as Langmuir circulation, current shears, etc.). These additional factors can change the volume of an oil slick significantly and thus the amount of tar that washes ashore. Mechanistically, some oil weathering processes (i.e., spreading and evaporation) are temperature dependant (Reed et al., 1999); thus, SST likely alters weathering rates. Oil slick dispersion due to the thinning of a slick, as a result of warmer temperatures increasing the rate of spreading and evaporation, could ultimately
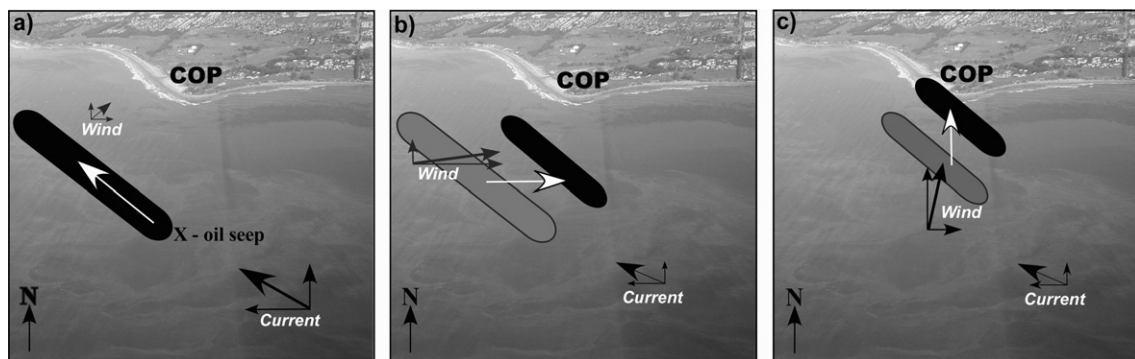

Fig. 5. Simplified schematic superimposed on aerial image of Coal Point showing sequence of conditions favorable for tar accumulation. Black arrow lengths represent surface speed and direction due to winds and currents. White arrows show oil slick transport direction. Black and gray ovals represent oil slick's current and former position, respectively. (a) Initially, currents near Coal Point (COP) transport oil slicks originating from marine hydrocarbon seeps (e.g., location 'X') northwest for conditions of light wind. (b) Winds to the East then transport the slick back towards COP. Absent a wind to the north component (c) the slick may miss COP.

decrease beach tar accumulation (i.e., we would expect SST to be inversely related to tar accumulation).

4.4. Source strength variations

In addition to environmental factors, some of the variability in M likely arises from source emission variability. It is known that seep gas emissions vary over a range of time scales, from second to decadal (Boles et al., 2001; Leifer and Boles, 2005). Few studies have looked at oil emissions; however, Leifer and Wilson (2007) showed a strong tidal influence on the oil emission from a seep with higher emissions during lower water levels. It is unknown if there is a seasonal variation in seep field oil emissions. One potential mechanism for a seasonal emission variation is via temperature-dependent oil viscosity changes in the shallow sediment near the seabed as a result of SBT changes. Oil viscosity is inversely correlated with temperature; therefore, high sea bottom temperatures in summer may result in greater oil emissions, and thus higher M. Our analyses, however, showed a significant negative correlation between SBT and $M(t)$. This cannot be explained physically and may be an artifact of an incomplete dataset. Other factors that also could lead to variability in emissions include aquifer pressure and earth tides, as well as geological factors related to oil and gas migration within the subsurface oil reservoir and along faults and fractures to the seabed.

4.5. Implications of studies on tar from natural marine seeps

Locally, the study of COP tar accumulation is important to the public whom regularly use COP beaches and to the Coal Oil Point Reserve Snowy Plover Program, whom monitors a dense nesting site for the threatened Western Snowy Plover, *Charadrius alexandrinus* (Lafferty, 2001). Our study has found a significant seasonal variation in COP beach tar with ten times more tar in summer than in winter. COP beaches are heavily used in summer and the nesting season for Snowy Plovers is March through September (Lafferty, 2001). Thus, better understanding of seasonal trends and causes of high tar accumulation could play a role in management plans for the endangered Snowy Plover. Further, absent an understanding of seasonal trends in tar accumulation near COP, an anthropogenic oil spill (from nearby shipping lanes or oil platforms) could be masked by the high summer tar deposits. This study has thus provided a method and a background value that can help distinguish between natural and anthropogenic beach tar accumulation at COP.

The complex oceanographic parameters influencing oil/tar transport in the coastal zone are lacking in most oil spill modeling programs. Our study used a natural and continuous oil spill source in coastal waters and natural beach tar accumulation to identify the coastal oceanographic parameters important for oil/tar transport and beach stranding. This type of study could not only help oil spill modelers with coastal parameters, but also inform oceanographers about advective processes in the coastal zone.

5. Conclusions

This paper describes a new and robust sampling method to quantify beach tar accumulation at one of the most heavily tarred beaches in North America. We have highly resolved beach tar mass repeatedly at COP using a tar size segregation method that encompasses the tar piece size range found in that area. Our method is standardized to the size ranges found at COP on designated transects and was designed to be repeated objectively by different surveyors. Our study found a seasonal variation in beach tar accumulation with an order of magnitude more tar accumulating on COP beaches during summer than during winter. The collection of 57 tar mass data points was sufficient to analyze tar accumulation with respect to environmental factors, while the dense sampling grid and survey area integration assured that tar at COP was well quantified and not dependant on a few very large tar pieces.

Although natural seeps introduce complexities, their long-term chronic nature and constrained geographic location provides advantages, particularly for long-term studies, for identifying important environmental variables to tar accumulation. The multiple regression analysis indicated that winds and swell are important factors influencing tar accumulation at COP. The remaining variation may be explained by other environmental factors not addressed in our study or in the stochastic nature of oil seep emissions.

Table of nomenclature

Variable	Units	Definition
D	cm	Diameter of tar piece surface area
f	n/a	Fraction of a circle to which tar piece surface area is equivalent
h	cm	Tar piece thickness
k	cm	Characteristic length of tar piece
M	kg	Total tar mass in survey area
m	g	Mass of individual tar pieces
r	cm	Radius of tar piece surface area
S	n/a	Tar piece size class
t	day	Time
u_c	cm s^{-1}	East-west surface current component
u_w	cm s^{-1}	East-west wind component
V	cm^3	Volume
v_c	cm s^{-1}	North-south surface current component
v_w	cm s^{-1}	North-south wind component
X	n/a	Transect
Y	n/a	Quadrat along transect
ρ_t	g cm^{-3}	Tar density

Acknowledgements

References

Allen, A.A., Schleuter, R.S., Mikolaj, P.G., 1970. Natural oil seepage at coal oil point, Santa Barbara, California. Science 170, 974–977.

Asuquo, F.E., 1991. Tar balls on Ibeno–Okposo beach of Southeast Nigeria. Mar. Pollut. Bull. 22 (3), 152–153.

Boles, J.R., Clark, J.F., Leifer, I., Washburn, L., 2001. Temporal variation in natural methane seep rate due to tides, Coal Oil Point area, California. J. Geophys. Res. – Oceans 106 (C11), 27,077–27,086.

Clester, S.M., Hornafius, J.S., Scepan, J., Estes, J.E., 1996. Quantification of the relationship between natural gas seepage rates and surface oil volume in the Santa Barbara Channel, (abstract). EOS (Am. Geophys. Union Trans.) 77 (46), F419.

Corbin, C.J., Singh, J.G., Ibiebele, D.D., 1993. Tar ball survey of six eastern Caribbean countries. Mar. Pollut. Bull. 26 (9), 482–486.

Fischer, P.J., 1977. Natural gas and oil seeps, Santa Barbara Basin, California. In: Welday, E.E. (Ed.), Natural gas and oil seeps, Santa Barbara Basin, California, . In: California Offshore Gas, Oil, and Tar Seeps. Calif. State Lands Comm., Sacramento, CA, pp. 1–62.

Fischer, P.J., Stevenson, A.J., 1973. Natural hydrocarbon seeps Santa Barbara basin. In: Fischer, P.J. (Ed.), Santa Barbara Channel Area Revisited Field Trip Guidebook. Am. Assoc. of Pet. Geol., Tulsa, Okla, pp. 17–28.

Gabche, C.E., Folack, J., Yongbi, G.C., 1998. Tar ball levels on some beaches in Cameroon. Mar. Pollut. Bull. 36 (7), 535–539.

Golik, A., 1982. The distribution and behavior of tar balls along the Israeli coast. Estuar., Coast. Shelf Sci. 15 (3), 267–274.

Harms, S., Winant, C.D., 1998. Characteristic patterns of the circulation in the Santa Barbara Channel. J. Geophys. Res. 103, 3041–3065.

Hartman, B., Hammond, D., 1981. The use of carbon and sulfur isotopes as correlation parameters for the source identification of beach tar in the southern California borderland. Geochim. Cosmochim. Acta 45, 309–319.

Henyey, T., Nardin, T., Nardin, B., 1977. In: Welday, E.E. (Ed.), Oil and tar seep studies on the shelves off southern California, Santa Monica Bay, California Offshore Gas Oil, and Tar Seeps. Calif. State Lands Comm., Sacramento, CA, pp. 63–109.

Hornafius, J.S., Quigley, D.C., Luyendyk, B.P., 1999. The world's most spectacular marine hydrocarbons seeps (Coal Oil Point, Santa Barbara Channel, California): quantification of emissions. J. Geophys. Res. – Oceans 104 (C9), 20,703–20,711.

Hostettler, F.D., Rosenbauer, R.J., Lorenson, T.D., Dougherty, J., 2004. Geochemical characterization of tarballs on beaches along the California coast: Part I – Shallow seepage impacting the Santa Barbara Channel Islands, Santa Cruz, Santa Rosa and San Miguel. Organic Geochem. 35, 725–746.

Hunt, J.M., 1996. Petroleum Geochemistry and Geology. W.H. Freeman & Co., New York, 743 pp.

Iliffe, T.M., Knap, A.H., 1979. The fate of stranded pelagic tar on a Bermuda beach. Mar. Pollut. Bull. 10 (7), 203–205.

Jokuty, P., Whiticar, S., Wang, Z., Fieldhouse, B., Fingas, M., 1999. A Catalogue of Crude Oil and Oil Product Properties for the Pacific Region. Wiley, Ottawa, ON, 264 pp.

Kvenvolden, K.A., Rosenbauer, R.J., Hostettler, F.D., Lorenson, T.D., 2000. Application of organic geochemistry to coastal tar residues from central California. Int. Geology Rev. 42, 1–14.

Lafferty, K., 2001. Disturbance to wintering western snowy plovers. Bio. Conser. 101, 315–325.

Landes, K.K., 1973. Mother nature as an oil polluter. Am. Assoc. Petroleum Geol. Bull. 57, 637–641.

Leifer, I., Luyendyk, B., Broderick, K., 2006a. Tracking an oil slick from multiple natural sources, Coal Oil Point, California. Marine Petroleum Geol. 23, 621–630.

Leifer, I., Boles, J., 2005. Turbine tent measurements of marine hydrocarbon seeps on subhourly time scales. J. Geophys. Res. 110 (C01006). doi:10.1020/2003JC002207.

Leifer, I., Wilson, K., 2007. The tidal influence on oil and gas emissions from an abandoned oil well: Nearshore, Summerland, California. Mar. Pollut. Bull., in press. doi:10.1016/j.marpolbul.2007.03.014.

Leifer, I., Luyendyk, B.P., Boles, J.R., Clark, J.F., 2006b. Natural marine seepage blowout: Contribution to atmospheric methane. Global Biogeochem. Cycles 20 (GB3008). doi:10.1029/2005GB00266.

Leifer, I., Boles, J.R., Luyendyk, B.P., Clark, J.F., 2004. Transient discharges from marine hydrocarbon seeps: Spatial and temporal variability. Environ. Geol. 46, 1038–1052. doi:10.1007/s00254-004-1091-3.

Lorenson, T.D., Dougherty, J.A., Hostettler, F.D., Rosenbauer, R.J., 2004. Natural seep inventory and identification for the county of Santa Barbara, California. Final Report, prepared for County of Santa Barbara, CA. <http://www.countyofsb.org/energy/information/NaturalSeepInventoryFinalReport.htm>.

Lorenson, T.D., Kvenvolden, K.A., Hostettler, F.D., Rosenbauer, R.J., Orange, D.L., Martin, J.B., 2002. Hydrocarbon geochemistry of cold seeps in the Monterey Bay National Marine Sanctuary. Mar. Geol. 181, 285–304.

Mearns, A.J., Simecek-Beatty, D., 2003. Longer-term weathering – Research needs in perspective. Spill Sci. Tech. Bull. 8 (2), 223–227.

Mertz, R.C., 1959. In: Determination of the quantity of oil substances on beaches and in nearshore waters, vol. 21. State Water Pollut. Control Board, Scramento, 45 pp.

NRC, 2003. Executive summary. Oil in the Sea III: Inputs, Fates, and Effects. National Academy of Sciences, Washington, DC.

Otero, E., Nieves, F., Corredor, J.E., 1987. Patterns of tar ball accumulation on a Lunate Coral Key at La Parguera, Puerto Rico. Carib. J. Sci. 23, 123–129.

Owens, E.H., 1999. SCAT – a 10-year review. In: Proceedings 22nd Arctic and Marine Oilspill Program (AMOP) Technical Seminar, Environment Canada, Calgary, Alberta, pp. 337–360.

Owens, E.H., Mauseth, G.S., Martin, C.A., Lamarche, A., Brown, J., 2002. Tar ball frequency data and analytical results from a long-term beach monitoring program. Mar. Pollut. Bull. 44, 770–780.

Quigley, D.C., Hornafius, S.J., Luyendyk, B.P., Clark, J.F., Washburn, L., 1999. Decrease in natural marine hydrocarbon seepage near Coal Oil Point, California associated with offshore oil production. Geology 27 (11), 1047–1050.

Reed, M., Johansen, O., Brandvik, P.J., Daling, P., Lewis, A., Fiocco, R., Mackay, D., Prentki, R., 1999. Oil spill modeling towards the close of the 20th century: overview of the state of the art. Spill Sci. Tech. Bull. 5 (1), 3–16.

Richardson, Q.B., Classen, J.A., Gijsbertha, E.M., 1987. Tar pollution monitoring in Curacao. Carib. J. Sci. 23 (1), 145–152.

Romero, G.C., Harvey, G.R., Atwood, D.K., 1981. Stranded tar on Florida beaches: september 1979–October 1980. Mar. Pollut. Bull. 12 (8), 280–284.

Sen Gupta, R., Fondekar, S.P., Alagarsamy, R., 1993. State of oil pollution in the Northern Arabian Sea after the 1991 Gulf Oil Spill. Mar. Pollut. Bull. 27, 85–91.

Shannon, L.V., Chapman, P., Eagle, G.A., McClurg, T.P., 1983. A comparative study of tar ball distribution and movement in two boundary current regimes: implications for oiling of beaches. Oil Petrochem. Pollut. 1 (4), 243–259.

Sokal, R.R., Rohlf, F.J., 1995. Biometry: the principles of statistics in biological research, third ed. W.H. Freeman and Co., New York, 887 pp.

Washburn, L., Clark, J.F., Kyriakidis, P., 2005. The spatial scales, distribution, and intensity of natural marine hydrocarbon seeps near Coal Oil Point, California. Marine Petroleum Geol. 22 (4), 569–578.